FLUX AND FLUENCE DETERMINATION USING THE MATERIAL SCRAPINGS APPROACH

MATERIALS

MICHAEL P. MANAHAN, Sr. and HASSAN S. BASHA
Pennsylvania State University, 231 Sackett Building
University Park, Pennsylvania 16802

Received February 7, 1990
Accepted for Publication June 20, 1990

The conventional approach to flux determination is to use high-purity dosimeters to characterize the neutron field. An alternative approach referred to as the material scrapings method is presented. Steel scrapings are cut from an in-service component and this material is used to measure the specific activity for various reactions. This approach enables the determination of the neutron flux and fluence incident on any component for which small chips of material can be safely obtained. The scrapings methodology was benchmarked by comparison with the results obtained using conventional dosimetry data from the San Onofre Nuclear Generation Station Unit 2.

Pseudo fast fluxes ($E > 1.0$ and 0.1 MeV) are calculated by combining the surveillance capsule dosimetry measured activities with the corresponding effective cross sections. The effective cross sections for the reactions of interest are calculated using the analytically determined neutron spectrum at the surveillance capsule position. After the evaluation and testing of the surveillance capsule were completed, scrapings were taken from a broken Charpy specimen. The pseudo fluxes for the $^{54}Fe(n,p)^{54}Mn$ and $^{58}Ni(n,p)^{58}Co$ reactions were calculated using the same cross sections as those used for the capsule dosimetry analysis. The pseudo fluxes determined using the scrapings dosimetry are within 5% of the corresponding surveillance capsule pseudo fluxes.

INTRODUCTION

Radiation damage to core internals, support structures, the pressure vessel, and other critical plant components must be evaluated to ensure safe operation through end-of-license (EOL) and during the plant life extension (PLEX) period. Most power plants have a pressure vessel surveillance program to monitor embrittlement through EOL. Niagara Mohawk[1] was the first utility to reencapsulate and reinsert an advanced boiling water reactor capsule for the purpose of generating PLEX data. The use of miniaturized specimen technology[2-8] and weld reconstitution[9] will be of great value to the utilities in generating vessel surveillance data during the life extension period. However, the scrapings technology can be used to generate PLEX data during each plant outage. In addition, the scrapings technology can provide data on the fluence and the mechanical behavior state for components such as reactor internals that would otherwise be difficult or impossible to obtain without destructively removing them from service. In cases where material data records have been lost, the scrapings approach would yield chemistry as well as flux data.

The most likely materials to be analyzed are ferritic and austenitic steels. Most of these classes of material contain sufficient minor alloying and impurity atoms to yield spectral dosimetry data. The scope of work for the present study includes the analysis of an American Society for Testing and Materials (ASTM) A533B steel from the San Onofre Nuclear Generating Station Unit 2 (SONGS)-2 97-deg surveillance capsule. This approach enables a comparison of the results obtained from scrapings taken from a Charpy specimen with the surveillance capsule dosimetry data. To the best of our knowledge, this is the first study of its kind to substantiate the scrapings approach on ferritic pressure vessel steel. Although the scrapings used in the present work were prepared in a controlled manner, we do not anticipate any increase in the uncertainty when the scrapings are removed from an in-service component. Of course, care must be exercised to ensure that the purity

of the material is maintained during cutting and handling.

BACKGROUND

The scrapings approach has been used in the past to measure the neutron flux at critical locations along the surface of the reactor pressure vessel (RPV) wall stainless steel liner. In 1981, Hegedues,[10] working for The Swiss Federal Institute for Reactor Research, used the scrapings sampling approach for fast neutron pseudo flux determination at the inner surface of an RPV. During shutdown, stainless steel scrapings, each weighing ~100 mg, were taken using a special boring machine, at several azimuthal locations near the core midplane. Chemical separation and neutron activation analyses were performed on the scrapings to determine their iron and niobium content. The material specific activities were used to determine the neutron flux at the inner surface of the RPV wall. Hegedues analyzed the neutron fluences obtained from the ^{93m}Nb and ^{54}Mn measurements. He reported a 10% difference between the ^{93m}Nb and ^{54}Mn pseudo fluences.

Belgian researchers also used the scrapings approach to determine the neutron flux and fluence at the BR-3 reactor[11] in an effort to enhance their surveillance program. In this study, dosimetry measurements were performed using chips cut from the thermal shield at several azimuthal locations near the core midplane and at several vessel wall locations near the nozzle centerline of the BR-3 reactor. A critical weld was also investigated at eight vertical elevations above the top of the thermal shield. Both physics dosimetry and chemical analyses were performed on the scrapings samples. The radial flux variation through the thermal shield and the RPV was determined using specific activities for the ^{54}Fe$(n,p)^{54}$Mn and ^{59}Co$(n,\gamma)^{60}$Co reactions. The pseudo fluxes agreed well with the transport calculated fluxes insofar as the radial flux distribution shape is concerned. The magnitudes of the transport calculated fast fluxes were higher than the pseudo fluxes. The average calculated to experimental (C/E) ratio varied from 1.10 to 1.15.

CONVENTIONAL FLUX CALCULATIONS

Fast neutron flux and fluence values with energies >0.1 MeV and >1.0 MeV at the SONGS-2 surveillance capsule, at the peak vessel flux position for the inner wall surface, one-quarter thickness ($\frac{1}{4}$ T), three-quarter thickness ($\frac{3}{4}$ T), and outer wall surface were determined as part of the surveillance capsule analysis. For the purpose of comparing the results with the scrapings approach, only the data at the capsule location are presented here. ASTM procedures were followed in the measurement of the dosimeter activities and calculation of the neutron flux and fluence.[12-23] The calculative details are described below.

Neutron Dosimetry

The SONGS-2 97-deg surveillance capsule contained 27 flux monitors. Nine monitors were located in each of three tensile monitor compartments. Each compartment contained two monitor housings. One housing contained aluminum-cobalt (Al-Co), uranium, titanium, iron, and sulfur flux monitors encapsulated in stainless steel sheaths (except for sulfur, which was encapsulated in quartz). The other housing contained Al-Co, uranium, nickel, and copper monitors within cadmium shielding to reduce the thermal neutrons. These cadmium shielded monitors were also encapsulated in stainless steel sheaths. A list of dosimeter reactions of interest is provided in Table I. This table excludes the sulfur dosimeter, whose isotope of interest has a half-life that is too short to provide useful data for this study.

Neutron Transport Analysis

The energy and spatial distribution of the neutron flux was calculated using the DOT 4.3 computer program.[24] DOT solves the Boltzmann transport equation in two-dimensional geometry using the method of discrete ordinates. Balance equations are solved for the density of particles moving along discrete directions in each cell of a two-dimensional mesh. Anisotropic scattering was treated using Legendre expansion. Third-order scattering P_3 and S_8 angular quadrature was used, i.e., neutrons travel in 48 directions (24 positive and 24 negative). Neutrons were divided into 47 groups with energies ranging from 17.3 MeV to 1×10^{-5} MeV. This 47-group structure is that of the Radiation

TABLE I

Dosimetry Reactions Used to Analyze the SONGS-2 Pseudo Fluxes

High-Purity Dosimeter Materials	Reaction	Threshold Energy (MeV)	Half-Life
Uranium	^{238}U$(n,f)^{137}$Cs	1.5	30.0 yr
Uranium	^{238}U$(n,f)^{144}$Ce	1.5	284 days
Uranium	^{238}U$(n,f)^{103}$Ru	1.5	40 days
Uranium	^{238}U$(n,f)^{95}$Zr	1.5	64.1 days
Nickel	^{58}Ni$(n,p)^{58}$Co	2.1	71.2 days
Iron	^{54}Fe$(n,p)^{54}$Mn	2.5	312.6 days
Titanium	^{46}Ti$(n,p)^{46}$Sc	3.9	83.9 days
Copper	^{63}Cu$(n,\alpha)^{60}$Co	6.1	5.27 yr
Al-Co	^{59}Co$(n,\gamma)^{60}$Co	Thermal	5.27 yr

Shielding Information Center Data Library BUGLE-80 (Ref. 25). The neutron absorption, scattering, and fission cross sections are those supplied in this library.

Both an r-θ and an r-z calculation were performed. Since >2000 meshes were modeled in the core alone, a computer code was written to determine what material lies in each core mesh. In the case of the r-z DOT run, the fuel assemblies are necessarily smeared into radial meshes. The material numbers are easily assigned manually since the material number input for this case is much easier to assign than in the r-θ case since each row is like that of the row immediately preceding it except at the radial extremities (corners) of the core. In these meshes, the number densities for the fuel and water regions were combined by appropriate weighting. Figure 1 shows the model used in the analysis.

The core shroud and core support barrel are Type 304 stainless steel. The vessel liner was modeled as Type 304 stainless steel. The RPV wall is SA533B steel. The reactor core was modeled as homogenized fuel rods, B_4C-Al_2O_3 absorber rods, and water. The water in the core region has a density consistent with the

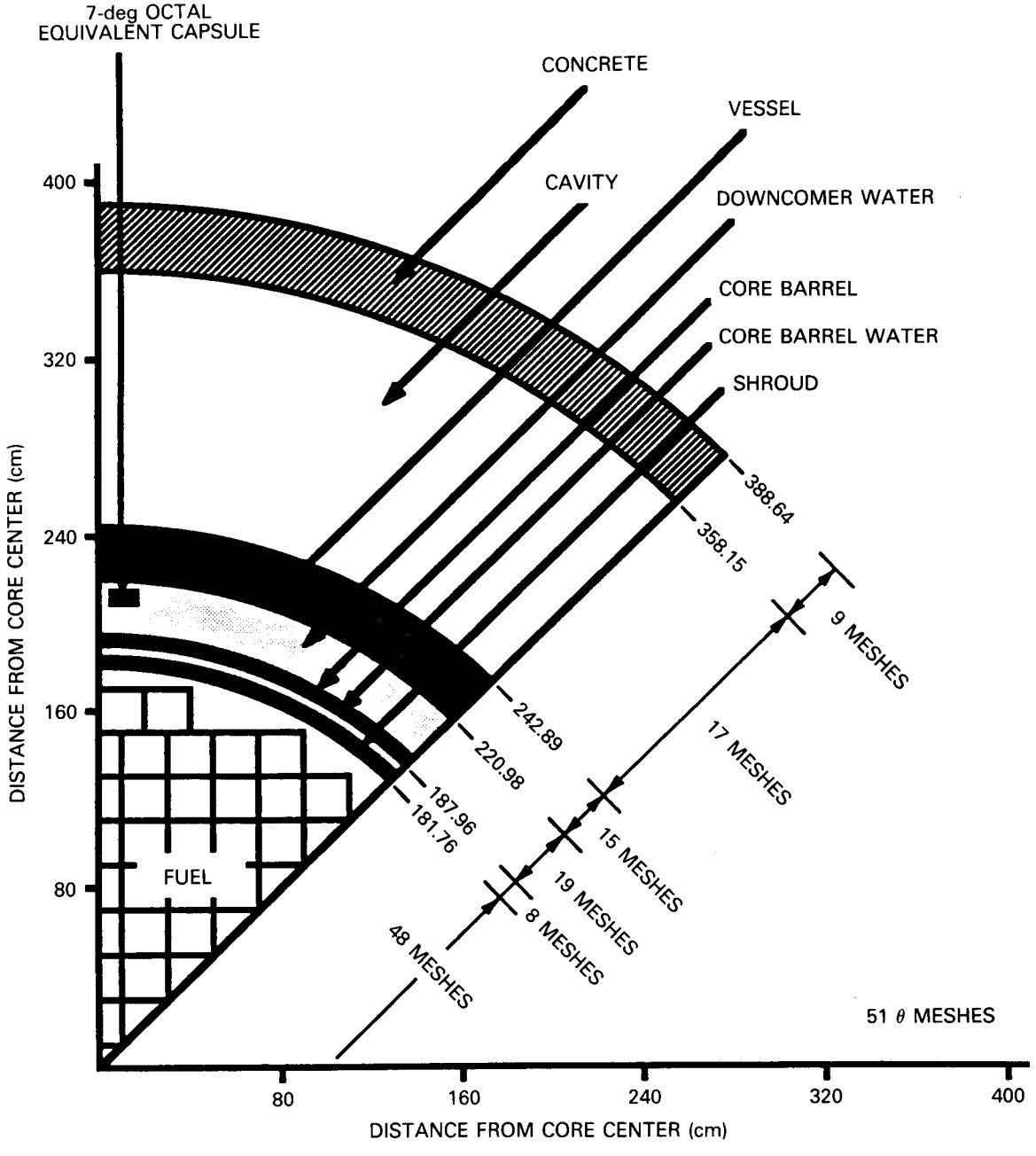

Fig. 1. Neutron transport r-θ model.

average coolant temperature in the core (583°F) at the operating pressure of 2250 psia. The water in the downcomer region outside the core barrel has a density consistent with the inlet coolant temperature (553°F) and operating pressure of 2250 psia. The coolant carried boron in solution at an average concentration of 462 g of boron per 10^6 g of water for cycles 1, 2, and 3. The boron concentration was averaged over the three cycles by burnup weighting the average boron concentration of each cycle. The fuel loading for cycle 3 was used to model the materials in the core region.

The number of neutrons per cubic centimetre per second originating in each mesh is proportional to the power generated in that mesh. Power generation in the meshes is calculated for both the r-θ and r-z DOT runs based on the number of pins whose centers lay in each mesh and on the power in these pins. A computer code was written to perform these calculations. The relative pin powers were that of the PDQ depletion analysis supplied by the utility. The pin powers and the axial power for each assembly were first averaged over each depletion step for all cycles using burnup weighting. Then, each cycle-averaged pin and axial power was averaged over all cycles by burnup weighting each cycle. The PDQ data were also used to obtain burnup weighting factors for determination of nu_{eff}, the average number of neutrons per fission. These same weights were used to calculate the effective fission spectrum.

Since the pin power model locates pin power centers and assigns pins to the appropriate meshes, an analysis was performed to estimate the maximum uncertainty introduced in this approach. For the meshing used in this analysis, 48% of the pins could potentially be impacted by the modeling approximation. If the pin centers were located at the farthest mesh corners, then the maximum impact on the fast flux due to source redistribution would be 1.8%. This is a result of the extremely fine mesh used in the r-θ plane in the core region. Therefore, this approximation is judged to have negligible effects on the flux prediction accuracy.

To determine a three-dimensional flux, separability was assumed and the results of the DOT r-θ and r-z runs were synthesized. The two synthesis approaches are described below. If we let

$$\phi(r,z,\theta) = C(r)\phi(r,\theta)\psi(r,z) \qquad (1)$$

and require for θ normalization that

$$\int_0^{2\pi} \frac{\phi(r,z,\theta)\,d\theta}{\int_0^{2\pi} d\theta} = \psi(r,z) \ , \qquad (2)$$

then

$$\int_0^{2\pi} \frac{C(r)\phi(r,\theta)\psi(r,z)\,d\theta}{2\pi} = \psi(r,z) \qquad (3)$$

and

$$C(r) = \frac{2\pi}{\int_0^{2\pi} \phi(r,\theta)\,d\theta} \ . \qquad (4)$$

In the case of z normalization, it was required that

$$\int_0^z \frac{\phi(r,z,\theta)\,dz}{\int_0^z dz} = \phi(r,\theta) \ , \qquad (5)$$

then

$$\int_0^z \frac{C(r)\phi(r,\theta)\psi(r,z)\,dz}{Z} = \phi(r,\theta) \qquad (6)$$

and

$$C(r) = \frac{Z}{\int_0^z \psi(r,z)\,dz} \ . \qquad (7)$$

A computer code, which reads the DOT output files, was used to perform the numerical integration of Eq. (7). This code also synthesized the fluxes at specific positions. These positions include the capsule locations, wall surface, $\frac{1}{4}$ T, and $\frac{3}{4}$ T in the vessel at desired locations (e.g., where the flux was the largest). In the analyses contained in this paper, the z normalization is used. We believe that the best geometric representation can be obtained using this model.

Empirical Determination of Flux

In a dosimeter irradiation experiment, the parameter that is actually measured is the activity of the dosimeter rather than the flux. To infer the flux from the activity, it is necessary to also know the energy dependence of the dosimeter cross section and the energy dependence of the flux at the dosimeter location. In this study, neutron transport analyses are performed that could be used to estimate the neutron energy spectra at the dosimeter locations. Thus, the "measured" or "pseudo fluxes" described in this paper are actually a combination of a measured activity and an analytically determined effective cross section from which the flux is determined.

The pseudo flux, accounting for decay between exposure and counting as well as power level fluctuation, is given by

$$\phi(E > E_c) = \frac{A}{N\sigma(E > E_c)C} \ , \qquad (8)$$

where

A = measured specific activity

E_c = cutoff energy

N = atom density of target nuclei

$\sigma(E > E_c)$ = effective cross section

$$\sigma(E > E_c) = \frac{\int_0^\infty \sigma(E)\phi(E)\,dE}{\int_{E_c}^\infty \phi(E)\,dE}$$

$$C = \sum_{n=1}^{K} f_n[1 - \exp(-\lambda t_i^n)]\exp(-\lambda t_w^n),$$

where

K = number of time intervals of constant flux

f_n = fractional power level during interval n

t_i^n = time length of the interval n irradiation

t_w^n = time between the end of interval n and counting.

To account for the effects of the cadmium cover, one obtains a modified dosimetry cross section $\sigma^*(E)$, which is

$$\sigma^*(E) = \sigma(E)\exp[-\Sigma_{CD}(E)X_{CD}] \ ,$$

where

$\Sigma_{CD}(E)$ = macroscopic cadmium removal cross section

X_{CD} = thickness of the cadmium filter.

The modified dosimetry cross section is substituted for the normal dosimetry cross section in Eq. (8), and the calculations proceed as before.

To determine the effective cross section $\sigma(E > E_c)$ to be used in the above calculations, the cross section as a function of energy must be known. The ENDF/B-V 640-group dosimetry cross-section library was used. A modified version of the National Bureau of Standards (NBS) DETAN code was used in the analysis to collapse the 640-group cross sections to a 47-group BUGLE-80 structure. The daily reactor operating history data supplied by the utility were used to compute the saturated activities of each dosimeter.

Spectral Unfolding

Since a measured activity is obtained for each type of dosimeter, a separate pseudo flux can be calculated at the monitor location for each dosimeter. Due to uncertainties in the counting, cross sections, geometric model, discrete ordinates approximation of the neutron transport equation, core and vessel eccentricity, and dosimeter impurities, the measured pseudo fluxes at a monitor location are all different (although from experience they are generally close in magnitude). A number of options exist for treatment of the different pseudo fluxes. One approach used in the past is to linearly average the pseudo fluxes and estimate the uncertainty by calculating the standard deviation about the mean. This is not, however, the preferred approach and can lead to an unintentional bias in the measured pseudo flux, particularly if one or more reactions included in the mean is inaccurate due to one or more of the reasons discussed above.

The preferred approach is, therefore, to adjust the flux spectrum and dosimetry data to bring the data into agreement, thus identifying potential outliers. The LSL-M2 code[26] was used for this purpose. Not only does LSL-M2 vary the flux spectrum, to obtain an optimized spectrum for all of the foils, but it also provides an estimate of the uncertainty in the fast flux based on the cumulative uncertainties propagated in the calculation. Thus, through the unfolding process, the best estimate of the fast flux and an uncertainty range for the fast flux is obtained at each monitored position.

The LSL-M2 code adjusts the transport calculated spectra using activation measurements. Inherent in the methodology is the estimation of uncertainties for the adjusted spectra based on corresponding uncertainties for the input data and the standard statistical procedure for the propagation of random errors. The spectral adjustment algorithm is a least-squares logarithmic statistical estimation procedure. Details regarding the mathematical background are provided in the LSL-M2 manual and elsewhere in the literature.

The cross-section file used as input to LSL-M2 was compiled from ENDF/B-V and the International Reactor Dosimetry Files. Cross-section covariances are obtained from standard cross-section files. At the present time, cross-section covariances are only available as variances and correlations between energy groups in a fairly coarse group structure. The fluence variances and covariances used are those of Maerker, which are supplied with the LSL-M2 code. A standard deviation of 5% was assumed for all nonfission reaction rates, and a standard deviation of 8% for all fission dosimeter reaction rates.

The BUGLE-80 47-group structure was collapsed to 20 groups for the spectral adjustment calculations. Fine group structure in spectral adjustment calculations is probably not warranted. The energy boundaries were chosen to coincide with the BUGLE-80 energy structure boundaries.

Neutron Flux C/E

The calculated-to-experimental (C/E) ratio is a convenient and useful measure of the uncertainty associated with the transport calculation. The C/E ratio can be determined as a function of position and, therefore, provide spatially dependent uncertainty estimates. It is only possible to determine a measured best-estimate or pseudo flux at the surveillance position (or scrapings location) by dividing dosimeter reaction activities by appropriate effective cross sections.

Several measures of the C/E ratio can be defined. The measures used in this analysis are

C/E = neutron transport calculated flux divided by the pseudo flux calculated from the transport spectrum

C^{adj}/E = adjusted transport flux divided by the pseudo flux calculated from the transport spectrum

C/E^{adj} = neutron transport calculated flux divided by the pseudo flux calculated from the adjusted spectrum

C^{adj}/E^{adj} = adjusted transport flux divided by the pseudo flux calculated from the adjusted spectrum.

RESULTS

The three-dimensional synthesized fluxes for the dosimetry capsules at three axial positions were calculated using the z-normalized neutron transport procedure described earlier. It was found that the z normalization method of three-dimensional flux synthesis provided results yielding C/E ratios closer to unity than did the θ normalization method. This is thought to be primarily due to the fact that the reactor geometry can be better represented in the r-θ model. In particular, in the z normalization, the r-θ analysis is performed at an axial elevation where the pin power is an average. The r-θ model captures all the other fuel bundle geometric detail. Therefore, to obtain the flux at various elevations, the r-θ solution need only be multiplied by the axial variation factor.

Conversely, in the θ normalization, the materials must be homogenized into the r-z plane and the θ variation is normalized to yield the three-dimensional flux. For most cases of practical interest, the flux magnitude cannot be obtained accurately due to the homogenization in the r-z plane. Therefore, we prefer to use the z normalization approach.

The ^{238}U fission product reactions showed more variation from the average than any other dosimeter reaction. In general, this can be due to impurities (e.g., ^{235}U, ^{233}Th, ^{239}Pu) in the ^{238}U foil. The procurement specification allowed up to 500 ppm of ^{235}U in the ^{238}U foils. These impurities would have the effect of altering the effective fission cross sections for the reactions. The ^{238}U powder was analyzed by thermal emission mass spectrometry and found to contain 0.039 at.% ^{235}U. The cross sections were modified to account for the impurity presence and the corrected activities were calculated. After correction, all the reactions yielded pseudo fluxes within the expected experimental uncertainty except for ^{95}Zr reaction. This reaction was not used in the spectral adjustment.

The peak azimuthal fast flux occurred at the octal equivalent azimuthal angle of 1.3 deg. The maximum axial flux occurred in the axial mesh falling between boundaries located between 30.0 and 33.0 in. below the core midplane (the center of this mesh is 31.5 in. below the core midplane). The azimuthal variation of the three-dimensional synthesized fluxes for $E > 1.0$ MeV at the RPV surface, $\frac{1}{4}$ T, and $\frac{3}{4}$ T are shown in Fig. 2. As anticipated, there is a general trend of the azimuthal profile to flatten as the radius increases. Plots of the radial flux profile near the bottom capsule compartment are shown in Fig. 3. The neutron fission

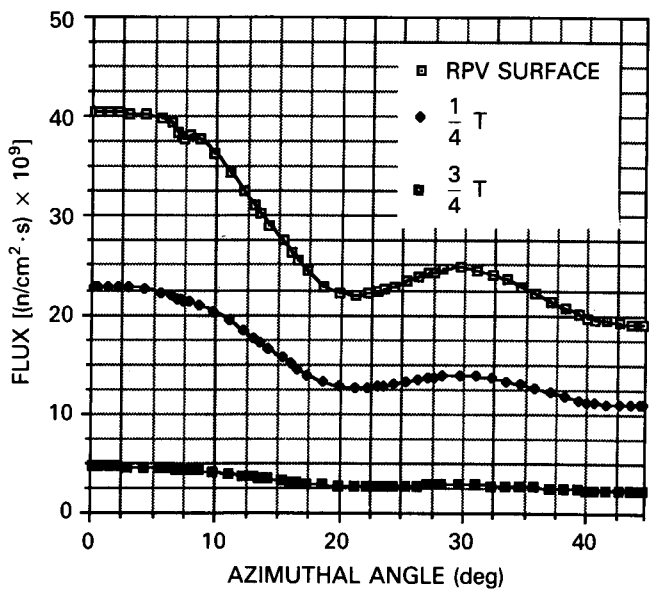

Fig. 2. Azimuthal flux variation at RPV surface, $\frac{1}{4}$ T, and $\frac{3}{4}$ T for $E > 1.0$ MeV at the peak axial elevation.

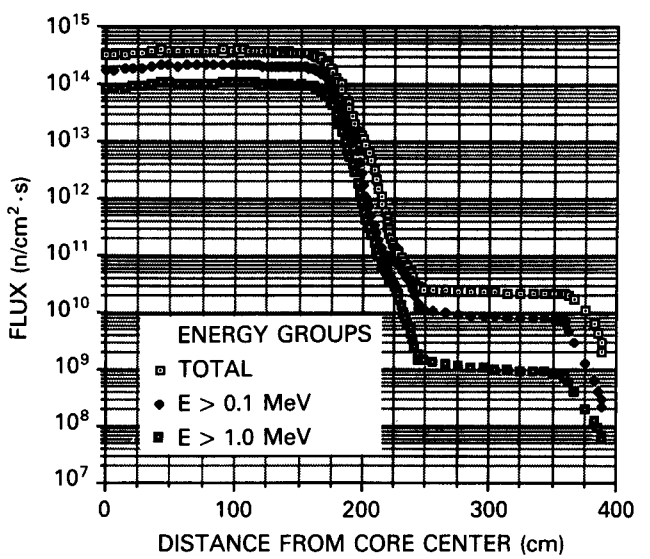

Fig. 3. Radial flux profile at 7-deg octal equivalent and 31.5 in. below the core midplane.

spectrum, core edge spectrum, and the capsule compartment spectrum are compared in Fig. 4. These spectra were normalized to contain one neutron above 1.0 MeV. As can be seen, the capsule spectrum is considerably harder than the fission and the core spectra.

The spectral adjustment was performed at all three axial positions in the capsule where dosimetry data were obtained. The spectral adjustment results in a standard deviation for the integral damage parameter of fast flux of ~4%. The standard deviation of the unadjusted spectra for the integral damage parameters of fast flux is ~12%. Hence, performing the spectral adjustment improved the transport integral damage parameter of fast flux by a factor of >3.

The adjusted fluxes were calculated using all the reactions except ^{95}Zr at the three compartment elevations for $E > 1.0$ MeV and $E > 0.1$ MeV. The C/E ratio for the dosimetry reactions at the core midplane are shown in Table II. The C/E ratio for the reactions considered is 0.73. Therefore, the uncertainty in the fast flux transport calculation is ~37% before adjustment and is 25% after adjustment for the SONGS-2 97-deg capsule. The C/E, C^{adj}/E, C/E^{adj}, and C^{adj}/E^{adj} are also shown in Table II. Analysis of these data indicates that the transport calculation is underpredicting the actual fast flux at the capsule. This is most likely due to several factors that contribute to the spectrum calculation such as core and vessel eccentricity, and cross-section errors.

The best estimate of the peak RPV surface, $\frac{1}{4}$ T, and $\frac{3}{4}$ T fluxes is obtained by applying a correction factor to the three-dimensional transport results to account for the fact that the transport result underpredicts the fast flux in the vicinity of the RPV. This factor is 1.25 and is defined as the average spectral adjusted pseudo flux divided by the average three-dimensional transport flux, both of which were determined at the center of the capsule (E^{adj}/C).

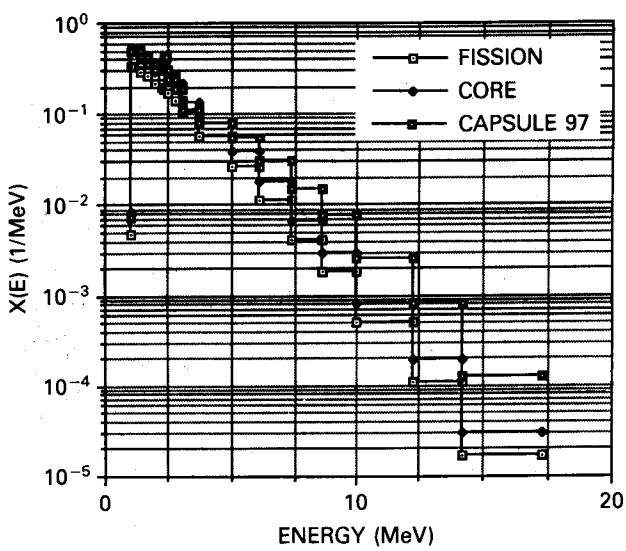

Fig. 4. Comparison of neutron fission spectrum, core edge spectrum, and capsule middle compartment spectrum for $E > 1.0$ MeV.

SCRAPINGS FLUX CALCULATIONS

Methodology

Charpy specimens from the SONGS-2 97-deg capsule were cleaned using concentrated HCl. This was done to remove any contamination from the Charpy specimen surface. Next, drilling chips were taken from the surface of the Charpy specimens using a hardened tool steel cutter. Care was exercised during cutting to avoid contaminating the ferritic steel chips.

The specific activity measurements for the scrapings were performed (as with the dosimetry wires) using a high-resolution gamma-ray spectrometer system. A Ge(Li) detector with a full-width at half-maximum resolution of 1.9 keV at 1332.5 keV, heavily shielded by lead to reduce background counts, was coupled to a 4096-channel pulse-height analyzer. Similar procedures to those used in the surveillance capsule dosimetry measurement were used.

Two counting measurements were performed on the Charpy scrapings. In the first measurement, the counting time was on the order of 5000 s, which was sufficient so that the uncertainty in the integrated photopeak area for the isotopes of interest was <5% for a 90% confidence level. However, because of high background due to the ^{60}Co in the scrapings, it was necessary to perform a second, longer count. In the second measurement, the scrapings were counted for 48 h. This was done to enhance the accuracy of our pseudo flux calculations and to see if other reactions of interest could be measured. Figure 5 shows the short-time counting data and Fig. 6 illustrates the long-time count. Only the ^{54}Mn, ^{58}Co, and ^{60}Co peaks could be resolved with reasonable accuracy.

TABLE II

Fast Flux ($E > 1.0$ MeV) C/E Ratios for the SONGS-2 97-deg Surveillance Capsule

Monitor	C/E	C^{adj}/E	C/E^{adj}	C^{adj}/E^{adj}
Iron	0.72	0.88	0.78	0.95
Nickel	0.69	0.85	0.76	0.93
Copper	0.76	0.93	0.79	0.97
Titanium	0.82	1.01	0.85	1.04
Cobalt	0.84	1.03	0.83	1.02
Cd/Co	0.75	0.92	0.76	0.93
^{238}U	0.65	0.79	0.82	1.09
Average	0.73	0.92	0.80	0.99

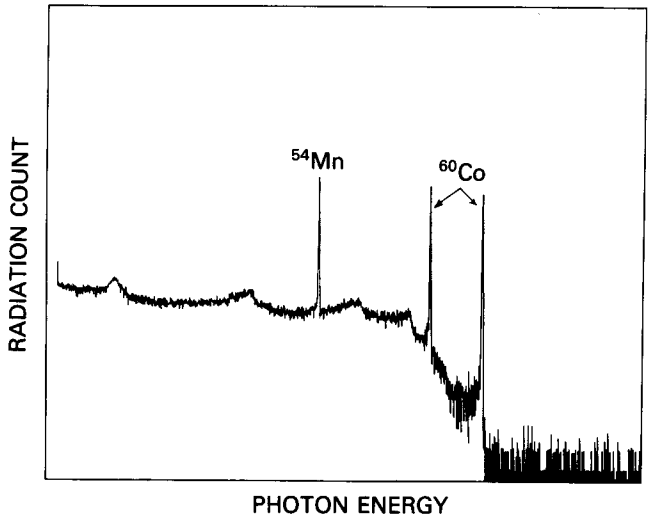

Fig. 5. Gamma-ray spectrum from multichannel analyzer for the short count of the Charpy specimen scrapings.

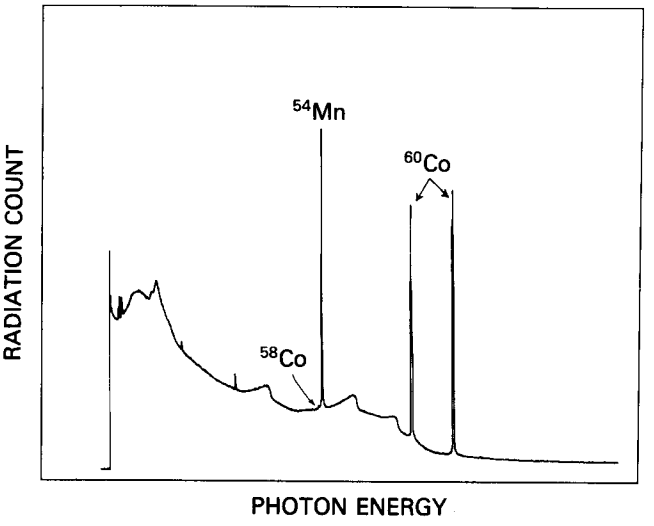

Fig. 6. Gamma-ray spectrum from multichannel analyzer for the long count of the Charpy specimen scrapings.

Chemical analysis was then performed on the Charpy specimen scrapings to determine the concentration of all the nuclei of interest (copper, nickel, iron, cobalt, and titanium). This analysis was performed using the method of inductively coupled plasma spectrometry (ICPS). This method is preferred since it is a bulk analysis technique as compared with X-ray fluorescence. Recent work performed by Battelle Memorial Institute using ICPS on many irradiated pressure vessel steel specimens yielded excellent reproducibility. Cross checks were also run on data determined using atomic absorption and it was found that the ICPS and the atomic absorption data compared well. Therefore, the ICPS was used to perform this analysis because of its accuracy and reproducibility. The results are shown in Table III.

Results and Benchmark Comparison

Table IV shows the activity measurements and the corresponding uncertainty for the long-term counts. The measured activities of the Charpy specimen scrapings were corrected to account for the time between reactor shutdown and counting and the saturation activities were determined. Only the ^{54}Fe$(n,p)^{54}$Mn and ^{58}Ni$(n,p)^{58}$Co reactions were used in the pseudo flux determination. The activity of the ^{58}Fe$(n,\gamma)^{59}$Fe reaction contained a large uncertainty and therefore was not analyzed. A decision was made not to analyze the ^{59}Co$(n,\gamma)^{60}$Co reaction because the isotope ^{60}Co can be produced from various different reactions through complex transmutation/decay chains.

The Charpy specimen scrapings pseudo fluxes were determined using the activities given in Table IV and the transport calculated effective cross sections. As shown in Table V, the Charpy specimen pseudo fluxes calculated using the ^{54}Fe$(n,p)^{54}$Mn and ^{58}Ni$(n,p)^{58}$Co reactions were within 5% of the corresponding surveillance capsule pseudo fluxes. This difference is most likely due to uncertainties in the chemical analysis results. The same neutron spectrum was used to calculate both pseudo fluxes. Based on the good agreement observed, the ability to accurately obtain fast flux data using dosimetry data obtained from ferritic steel scrapings has been demonstrated. Future work should focus on technology development to yield spectral dosimetry data.

SUMMARY AND CONCLUSIONS

Pseudo fluxes were first calculated using pressurized water reactor surveillance capsule dosimetry data.

TABLE III

Chemical Analysis Results for the Base Metal Specimens from the SONGS-2 97-deg Surveillance Capsule

Elements	Base Metal Composition (wt%)	
	Capsule	Baseline
Copper	0.100	0.10
Nickel	0.593	0.60
Phosphorus	0.0115	0.005
Chromium	0.204	0.18
Molybdenum	0.548	0.58
Vanadium	<0.025	0.003
Manganese	1.417	1.43
Cobalt	0.008	0.012

TABLE IV

Activities and Uncertainties for Charpy Specimen Scrapings

Reaction	Threshold Energy (MeV)	Half-Life	Activity (μC)	Uncertainty (%)
$^{58}Ni(n,p)^{58}Co$	2.1	71.2 days	2.39×10^{-3}	±0.91
$^{54}Fe(n,p)^{54}Mn$	2.5	312.6 days	1.04	±1.75
$^{59}Co(n,\gamma)^{60}Co$	Thermal	5.27 yr	1.29	±1.55
$^{58}Fe(n,\gamma)^{59}Fe$	Thermal	42 days	1.62×10^{-3}	±57.07

TABLE V

Fast Flux ($E > 1.0$ MeV) Ratios of the Surveillance Capsule Flux to the Flux Determined Using Charpy Specimen Scrapings

Reaction	ϕ^a/ϕ^b	Difference (%)
$^{54}Fe(n,p)^{54}Mn$	1.0475	4.75
$^{58}Ni(n,p)^{58}Co$	1.0515	5.15

[a]Neutron flux determined from the surveillance capsule radiometric monitors.

[b]Neutron flux determined from the Charpy specimen scrapings samples.

This was done by combining the measured activities with effective cross sections that were determined using analytically calculated neutron spectra at the capsule. Then, scrapings were taken from the surface of a Charpy specimen that came from the same surveillance capsule. Specific activity measurements were performed on the scraping samples. The pseudo fluxes for the scrapings were determined using the same calculated spectrum as was used for the capsule dosimetry analysis. The Charpy scrapings pseudo fluxes calculated using the $^{54}Fe(n,p)^{54}Mn$ and $^{58}Ni(n,p)^{58}Co$ reactions were within 5% of the corresponding pseudo fluxes calculated using conventional dosimetry.

This study demonstrates that scrapings obtained from an irradiated steel specimen can provide accurate estimates of the pseudo flux. While the scrapings results obtained in this study compare favorably with the surveillance capsule results, more accurate flux data can be obtained in the future if more spectral reactions, which cover the entire neutron energy spectrum, could be obtained. This would provide the necessary data to perform spectral unfolding to reduce the uncertainty in the calculated flux. This is desirable since spectral unfolding can reduce the uncertainty in the integrated fast flux by as much as a factor of 3.

ACKNOWLEDGMENTS

The authors wish to thank J. Talnagi from OSU-NRL for his assistance in preparation of the scraping samples and the activity counting measurements. We would also like to acknowledge Phil Brashear and Gerry Stevenson from Southern California Edison Company for allowing us to use their specimens and transport data to perform this work.

REFERENCES

1. M. P. MANAHAN and C. CHARLES, "A Generalized Methodology for Obtaining Quantitative Charpy Data from Test Specimens of Nonstandard Dimensions," *J. Nucl. Technol.*, **90**, 245 (1990).

2. B. MAJUMDAR, C. E. JASKE, and M. P. MANAHAN, "Determining Creep-Crack-Growth Behavior Using Miniature Specimens," *Int. J. Fracture Mechanics* (in press).

3. M. P. MANAHAN, R. KOHLI, J. SANTUCCI, and P. SIPUSH, "A Phenomenological Investigation of In-Reactor Cracking of Type 304 Stainless Steel Control Rod Cladding," *J. Nucl. Eng. Design*, **113**, 297 (1989).

4. M. P. MANAHAN, A. S. ARGON, and O. K. HARLING, "The Development of a Miniaturized Disk Bend Test for the Determination of Postirradiation Mechanical Properties," *J. Nucl. Mater.*, **103 & 104**, 1545 (Aug. 1981).

5. M. P. MANAHAN, "Determining Plane Strain Fracture Toughness and the Integral for Solid Materials Using Stress Field Modified Miniature Specimens," U.S. Patent Application (Jan. 1988).

6. M. P. MANAHAN, "Determining Fracture Mode Transition Behavior of Solid Materials Using Miniature Specimens," U.S. Patent Application (Jan. 1988).

7. M. P. MANAHAN, A. S. ARGON, and O. K. HARLING, "Determining Mechanical Behavior of Solid Materials Using Miniature Specimens," U.S. Patent Number 4.567.774 (Feb. 4, 1988).

8. M. P. MANAHAN, "Surveillance Capsules A′ and C′ for Nine Mile Point Unit 1," Final Report from Battelle Memorial Institute to Niagara Mohawk Power Corporation (Sep. 1987).

9. "Guide for the Reconstitution of Irradiated Charpy Specimens," ASTM E New Standard, American Society for Testing and Materials (1990).

10. F. HEGEDUES, "Fast Neutron Dosimetry of the Scraping Sampling Method," *Proc. 5th ASTM-Euratom Symp. Reactor Dosimetry* (1984).

11. A. FABRY et al., "Improvement of LWR Pressure Vessel Steel Embrittlement Surveillance (1982–1983), Progress Report on Belgian Activities in Cooperation with the USNRC and Other R&D Programs," *Proc. 5th ASTM-Euratom Symp. Reactor Dosimetry* (1984).

12. "Practice for Conducting Surveillance Tests for Light-Water Cooled Nuclear Power Reactor Vessels," ASTM E185, American Society for Testing and Materials (1990).

13. "Practice for Effects of High-Energy Neutron Radiation on the Mechanical Properties of Metallic Materials," ASTM E184, American Society for Testing and Materials (1990).

14. "Method for Determining Neutron Flux, Fluence, and Spectra by Radioactivation Techniques," ASTM E261, American Society for Testing and Materials (1990).

15. "Method for Determining Thermal Neutron Flux by Radioactivation Techniques," ASTM E262, American Society for Testing and Materials (1990).

16. "Method for Determining Fast-Neutron Flux Density by Radioactivation of Iron," ASTM E263, American Society for Testing and Materials (1990).

17. "Method for Determining Fast-Neutron Flux Density by Radioactivation of Nickel," ASTM E264, American Society for Testing and Materials (1990).

18. "Method for Determining Fast-Neutron Flux Density by Radioactivation of Copper," ASTM E523, American Society for Testing and Materials (1990).

19. "Guide for Application of Neutron Transport Methods for Reactor Vessel Surveillance," ASTM E482, American Society for Testing and Materials (1990).

20. "Application of Neutron Spectrum Adjustment Methods in Reactor Surveillance," ASTM E944, American Society for Testing and Materials (1990).

21. "Method for Measuring Reaction Rates by Radioactivation of Uranium-238," ASTM E704, American Society for Testing and Materials (1990).

22. "Method for Measuring Reaction Rates by Radioactivation of Neptunium-237," ASTM E705, American Society for Testing and Materials (1990).

23. "Recommended Practice for Extrapolating Reactor Vessel Surveillance Dosimetry Results," ASTM E560, American Society for Testing and Materials (1990).

24. DOT IV, One- and Two-Dimensional Neutron-Photon Transport Code, "DOT IV Version 4.3," ORNL-5851, Oak Ridge National Laboratory (1982).

25. "Bugle 80 Coupled 47 Neutron, 20 Gamma, P_3 Cross-Section Library for LWR Shredding Calculations," DLC-75, Oak Ridge National Laboratory (1980).

26. "LSL-M2 Least-Squares Logarithmic Adjustment of Neutron Spectra," PSR-233 MICRO, Radiation Shielding Information Center, Oak Ridge National Laboratory (Oct. 1986).

Michael P. Manahan, Sr. (BS, mathematics, and BA, physics, Michigan State University, 1975; MS, reactor physics, Columbia University, 1978; ScD, nuclear materials engineering, Massachusetts Institute of Technology, 1982) is an associate professor of nuclear engineering at Pennsylvania State University (PSU). His research interests include plant life extension, miniaturized specimen technology, radiation damage in materials, radiation field measurement technology, radiation transport analysis, pressure vessel surveillance, and computer-based technology management.

Hassan S. Basha (BSc, nuclear engineering, University of Michigan, 1986; MSc, nuclear engineering, Ohio State University, 1989) is a PhD candidate and research assistant in the nuclear engineering department at PSU. His current interests include neutron transport and Monte Carlo calculations, reactor dosimetry and shielding analysis, and boron capture therapy.